The Astrophysical Journal, 795:18 (7pp), 2014 November 1 doi:10.1088/0004-637X/795/1/18

ENERGY PROPAGATION BY TRANSVERSE WAVES IN MULTIPLE FLUX TUBE SYSTEMS USING FILLING FACTORS

T. Van Doorsselaere[1], S. E. Gijsen[1], J. Andries[2], and G. Verth[3]
[1] Centre for mathematical Plasma Astrophysics, Mathematics Department, KU Leuven, Celestijnenlaan 200B bus 2400, B-3001 Leuven, Belgium; tom.vandoorsselaere@wis.kuleuven.be, stief.gijsen@wis.kuleuven.be
[2] Solar-Terrestrial Center of Excellence, Royal Observatory of Belgium, Ringlaan 3, B-1180 Brussels, Belgium; jesse.andries@oma.be
[3] Solar Physics and Space Plasma Research Centre (SP^{2}RC), The University of Sheffield, Hicks Building, Hounsfield Road, Sheffield S3 7RH, UK; g.verth@sheffield.ac.uk
Received 2014 March 26; accepted 2014 September 2; published 2014 October 9

ABSTRACT

In the last few years, it has been found that transverse waves are present at all times in coronal loops or spicules. Their energy has been estimated with an expression derived for bulk Alfvén waves in homogeneous media, with correspondingly uniform wave energy density and flux. The kink mode, however, is localized in space with the energy density and flux dependent on the position in the cross-sectional plane. The more relevant quantities for the kink mode are the integrals of the energy density and flux over the cross-sectional plane. The present paper provides an approximation to the energy propagated by kink modes in an ensemble of flux tubes by means of combining the analysis of single flux tube kink oscillations with a filling factor for the tube cross-sectional area. This finally allows one to compare the expressions for energy flux of Alfvén waves with an ensemble of kink waves. We find that the correction factor for the energy in kink waves, compared to the bulk Alfvén waves, is between f and $2f$, where f is the density filling factor of the ensemble of flux tubes.

Key words: plasmas – Sun: oscillations – waves

Online-only material: color figure

1. INTRODUCTION

For the past fifteen years, we have observed many examples of transverse waves in the solar corona. The first to be discovered were the standing transverse waves in coronal loops, after a flare (Schrijver et al. 1999; Aschwanden et al. 1999). Six years ago, it was discovered that low-amplitude propagating transverse waves are omnipresent in solar coronal loops (Tomczyk et al. 2007; Tomczyk & McIntosh 2009). This discovery was later confirmed by McIntosh et al. (2011) using imaging data of *SDO*/AIA. *Hinode*/XRT has also observed transverse waves in coronal jets (Cirtain et al. 2007; Vasheghani Farahani et al. 2009).

Also, in the chromosphere, we have known of the presence of transverse waves in spicules for a long time (e.g., Pasachoff et al. 1968; Zaqarashvili et al. 2007). This was recently brought to prominence again by De Pontieu et al. (2007), who showed that practically all spicules show transverse motions. It was observationally shown by He et al. (2009a, 2009b) and Okamoto & De Pontieu (2011) that these waves are propagating transverse waves as well. Moreover, it was claimed that transverse waves have been observed with *Hinode*/SOT in photospheric pores (Fujimura & Tsuneta 2009), but it was recently demonstrated that these observations could also be interpreted as axisymmetric slow waves (Moreels & Van Doorsselaere 2013).

The authors of some of the above articles have interpreted their observations of transverse waves in terms of Alfvén waves. However, this was not backed up by theorists (e.g., Erdélyi & Fedun 2007; Van Doorsselaere et al. 2008a; Pascoe et al. 2010), who claimed that these waves are better interpreted as kink waves (or surface Alfvén waves, Goossens et al. 2012a), in line with the interpretation of standing transverse waves (Nakariakov et al. 1999). In the kink wave description, the plasma structuring across the magnetic field is considered important for the wave properties and taken into account in the physical model. While the magnetic tension is still the driving force (Goossens et al. 2009) and a large vorticity component is present (Goossens et al. 2012a), the velocity field is no longer divergence free.

Despite the modeling uncertainties, the observed transverse oscillations have received a lot of attention from theorists and observers alike, because they proved an excellent tool to perform remote sensing of the solar corona. This technique is called coronal seismology, in which observed wave properties are compared to models of waves in order to gain insight into the physical properties of the background plasma (chromospheric spicules or coronal loops). The standing transverse waves have been successfully used to measure the coronal magnetic field (e.g., Nakariakov & Ofman 2001; Van Doorsselaere et al. 2008b), density scale height (e.g., Andries et al. 2005), cross-field structuring (e.g., Goossens et al. 2002, 2008; Aschwanden et al. 2003) and Alfvén speed (e.g., Arregui et al. 2007; Asensio Ramos & Arregui 2013). Also, since their discovery in 2007, the propagating transverse waves have been equally well exploited to measure the determining loop properties (e.g., Verth et al. 2010; Goossens et al. 2012b; Verwichte et al. 2013).

Aside from the seismological applications, the propagating transverse waves are important players in the coronal heating problem, because they propagate energy from the photosphere (where the scattering of p-modes in bundles of flux tubes has also been studied, e.g., Bogdan & Zweibel 1987) through the chromosphere and the corona to the solar wind, where they could dissipate due to their turbulent behavior (e.g., Verdini et al. 2012), and could be used as an extra driver mechanism for the solar wind (e.g., van der Holst et al. 2014). In this light, some of the recent works have estimated the wave energy in the transverse waves in the chromosphere and corona using observational wave properties. Some of these studies came to the conclusion that the waves could carry a significant part of the energy budget required to heat the solar corona, thereby solving the decade-old problem. However, as explained above, these works interpreted the transverse waves as bulk Alfvén waves in a homogeneous medium. It was argued by Van Doorsselaere et al.

(2008a), among others, that the waves should be modeled as kink waves, taking into account the plasma structuring perpendicular to the magnetic field.

Kink waves in cylindrical, field-aligned configurations were first mathematically described by Zaitsev & Stepanov (1975), Wilson (1979, 1980), and Spruit (1982). Edwin & Roberts (1983) made a very clear spectral classification of waves in a cylindrical, field-aligned configuration, that included the description of transverse waves on an overdense structure. Goossens et al. (2009, 2012a) showed that these kink waves are comparable to surface Alfvén waves (e.g., Wentzel 1979a, 1979b), because the main restoring force is the magnetic tension and the vorticity is contained at the discrete surface. Surface Alfvén waves are different from textbook bulk Alfvén waves, because they are confined to the density structure in which they live.

Naturally, the confinement of kink waves also has consequences for the localization of the energy. For bulk Alfvén waves, the energy is uniformly distributed in space and is propagated with the Alfvén speed. For kink waves, the energy is mostly confined to the density structure, with evanescent tails for larger distances from the structure. Thus, in order to estimate the energy flux in kink waves, one should look at the spatially averaged total energy, rather than the energy density as one would do for the bulk Alfvén waves. The phase speed of the kink mode is the kink speed, which is a weighted average of the internal and external Alfvén speeds.

The spatial distribution and total energy (integrated over the cross-section) for kink modes was calculated in detail by Goossens et al. (2013a) for a single flux tube. However, it has been shown by De Pontieu et al. (2007), McIntosh et al. (2011), and Morton et al. (2013) that transverse waves often live in an ensemble of chromospheric or coronal flux tubes. Because the kink wave energy is localized to the flux tubes, the propagated energy (averaged over the cross-section) will be changed compared to the energy of bulk Alfvén waves.

Therefore, we will extend the calculations performed by Goossens et al. (2013a) to systems of multiple flux tubes. We will connect the spacing between the multiple flux tubes to the filling factor. In the end, we aim to obtain a formula that computes the average energy flux using basic observable quantities.

2. FILLING FACTOR

Let us consider a bundle of N flux tubes with length L, where the ith tube has a radius R_i. The bundle of flux tubes is embedded in a cylindrical volume with radius $\mathcal{R}$. A possible configuration is shown in Figure 1. We will denote the density between the flux tubes as ρ_e ("external", indicated with yellow in Figure 1) and the density inside the flux tubes as ρ_i ("internal," indicated with red in Figure 1).

We define the filling factor, f, as the ratio of the flux tube volume to the total volume of the region containing the flux tubes (including the "empty" space between the flux tubes). Using the current notations, the filling factor, f, can be calculated as

$$f = \frac{\text{volume loops}}{\text{total volume}} = \frac{\sum_{i=1}^{N} \pi R_i^2 L}{\pi \mathcal{R}^2 L} = \frac{\sum_{i=1}^{N} R_i^2}{\mathcal{R}^2}. \quad (1)$$

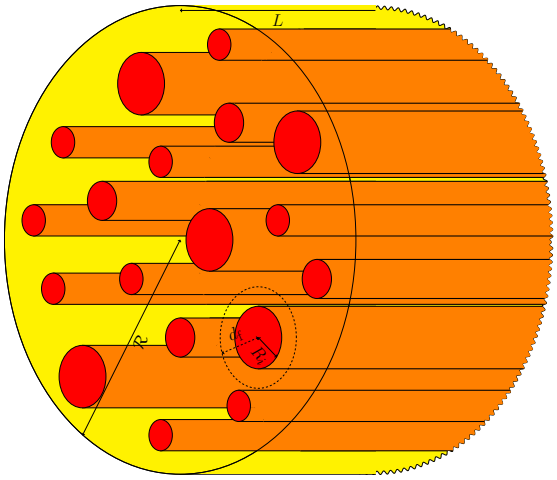

Figure 1. Example of the configuration that is used for the calculation of the filling factor, f. The considered volume is colored in yellow (low density), and the strands are drawn in red/orange (high density). The cylinder with radius d_f is also shown.

(A color version of this figure is available in the online journal.)

We can define a radius d_f of a circular cross-sectional area that is equal to the average area "belonging" to a single flux tube. By definition, d_f relates to the filling factor as

$$f = \frac{R^2}{d_f^2}. \quad (2)$$

Though it is clearly a measure for the average distance between the loops, such a relation can only be made explicit in a limited number of simple loop distribution models. For example, in the regular distributions depicted in Figure 2, $d_f = a/\sqrt{\pi}$, with a as the fixed center-to-center nearest neighbor distance. The definition of d_f is effectively the two-dimensional (2D) analog of defining the mean distance between particles using the number density.

Now, we concentrate on the volume with radius d_f only containing the loop with radius R. Using the definition of d_f (Equation (2)), we can introduce a new parameter, $\alpha_f = d_f/R$, that relates to the parameter α used by Goossens et al. (2013a). It is straightforward to relate α_f to the filling factor, f:

$$f = \frac{R^2}{d_f^2} = \frac{R^2}{\alpha_f^2 R^2} = \frac{1}{\alpha_f^2}, \quad (3)$$

and so

$$\alpha_f = \frac{1}{\sqrt{f}} = f^{-1/2}. \quad (4)$$

3. PROPAGATION OF ENERGY

3.1. Bulk Alfvén Waves

In the recent literature, the energy in observed transverse motions is often estimated using the formula for the energy of bulk Alfvén waves (denoted with the subscript bAw). Bulk Alfvén waves are the classical, textbook Alfvén waves that live in a homogeneous plasma with a homogeneous magnetic field. For those waves, the energy density is equal everywhere, and the propagation is along the magnetic field. These particular solutions only exist in a homogeneous plasma and any inhomogeneity would modify them.

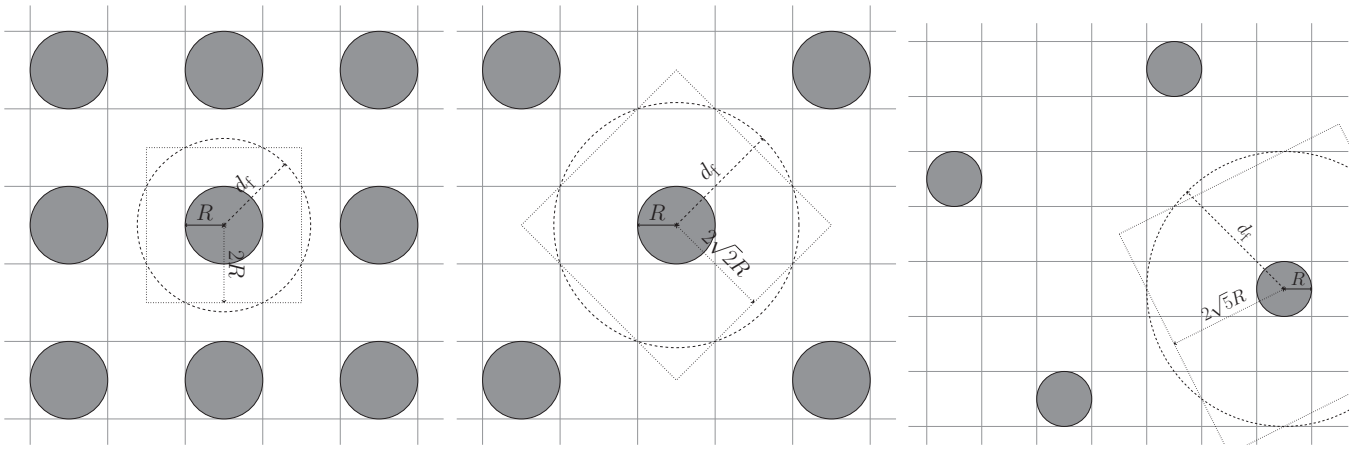

Figure 2. Three possible configurations of loops that allow for an observed interloop spacing of one loop in both the horizontal and vertical direction. The filling factors for the systems are (from left to right) 20%, 10%, and 4%.

Following textbooks (e.g., Walker 2005), the energy density, ε (with the physical units of J m^{-3}), can be calculated as

$$\varepsilon_{\rm bAw} = \frac{1}{2}\rho(\boldsymbol{v}\cdot\boldsymbol{v}^*) = \frac{1}{2}\rho w^2, \tag{5}$$

where ρ is the (uniform) density, $\boldsymbol{v}$ is the velocity perturbation, * is the complex conjugation, and w is the velocity amplitude. In this formula, the energy density has been averaged over a period and wavelength.

Let us return to the cylinder with radius $d_{\rm f}$, uniformly filled with a plasma of mean density ρ. If the whole volume of this plasma cylinder was filled with bulk Alfvén waves, then the total energy, E, in this volume would be given by

$$\begin{aligned} E_{\rm bAw} &= \int_{z=0}^{L} dz \int_{\phi=0}^{2\pi} d\phi \int_{r=0}^{d_{\rm f}} \frac{1}{2}\rho w^2 r\, dr, \\ &= \pi d_{\rm f}^2 L \frac{1}{2}\rho w^2, \\ &= V\frac{1}{2}\rho w^2, \end{aligned} \tag{6}$$

where we have used the expression for the energy density (Equation (5)) and have defined the volume $V = \pi d_{\rm f}^2 L$.

3.2. Kink Waves

It has been suggested that the observed transverse waves may be better described with the kink wave formalism (e.g., Van Doorsselaere et al. 2008a). Kink waves in field-aligned magnetic cylinders were first described by Zaitsev & Stepanov (1975). A recent investigation calculated that they are mainly driven by the magnetic tension force (Goossens et al. 2009) and can thus be considered as surface Alfvén waves, because a large vorticity is concentrated in the flux tube edge (Goossens et al. 2012a).

In a kink wave formalism, the MHD waves (using an azimuthal wave number $m = 1$) are described around an overdense magnetic cylinder that is aligned with the magnetic field. In this description, the plasma perturbations are given in terms of Bessel functions. The perturbations are concentrated around the flux tube and decay rapidly when going to larger radii.

The energy density and flux of kink waves in overdense flux tubes was recently calculated by Goossens et al. (2013a, 2013b). Using the long-wavelength limit, it is possible to compute the energy density, $\varepsilon_{\rm Kw,i}$ (averaged over one period and one wavelength), in the internal region of the flux tubes as

$$\varepsilon_{\rm Kw,i} = \frac{1}{4}\rho_{\rm i}\frac{v_{\rm k}^2 + v_{\rm Ai}^2}{v_{\rm k}^2} w^2, \tag{7}$$

by combining their Equations (23) and (31). They used the notation $< TE >_{\rm i/e}$ for the energy density $\varepsilon_{\rm Kw,i/e}$. Here, we have used the definition for the kink speed, $v_{\rm k}$, and Alfvén speed, $v_{\rm A}$,

$$v_{\rm k}^2 = \frac{\rho_{\rm i} v_{\rm Ai}^2 + \rho_{\rm e} v_{\rm Ae}^2}{\rho_{\rm i} + \rho_{\rm e}}, \quad v_{\rm A}^2 = \frac{B^2}{\mu\rho}. \tag{8}$$

The expression for the energy density in the external region, $\varepsilon_{\rm Kw,e}$, still contains a spatial dependence on the Bessel function:

$$\varepsilon_{\rm Kw,e} = \frac{1}{4}\rho_{\rm e}\frac{v_{\rm k}^2 + v_{\rm Ae}^2}{v_{\rm k}^2} w^2 \left(\frac{R}{r}\right)^4, \tag{9}$$

where r is the radial coordinate. We corrected the typo, pointed out in Goossens et al. (2013b), in Equation (27) from Goossens et al. (2013a) and immediately applied the long-wavelength limit to approximate the Bessel function.

The total energy, $E_{\rm Kw}$, for a kink wave (Kw) in the cylindrical region with radius $d_{\rm f} = \alpha_{\rm f} R$ surrounding the cylinder with radius R is thus

$$\begin{aligned} E_{\rm Kw} &= \int_{z=0}^{L} dz \int_{\phi=0}^{2\pi} d\phi \int_{r=0}^{R} \varepsilon_{\rm Kw,i} r\, dr \\ &\quad + \int_{z=0}^{L} dz \int_{\phi=0}^{2\pi} d\phi \int_{r=R}^{d_{\rm f}} \varepsilon_{\rm Kw,e} r\, dr \\ &= 2\pi L \left\{ \frac{1}{4}\rho_{\rm i}\frac{v_{\rm k}^2 + v_{\rm Ai}^2}{v_{\rm k}^2} w^2 \frac{R^2}{2} \right. \\ &\quad \left. + \frac{1}{4}\rho_{\rm e}\frac{v_{\rm k}^2 + v_{\rm Ae}^2}{v_{\rm k}^2} w^2 \frac{R^2}{2}\frac{\alpha_{\rm f}^2 - 1}{\alpha_{\rm f}^2} \right\} \\ &= 2\pi L \frac{1}{8} R^2 w^2 \left[\rho_{\rm i}\frac{v_{\rm k}^2 + v_{\rm Ai}^2}{v_{\rm k}^2} + \rho_{\rm e}\frac{v_{\rm k}^2 + v_{\rm Ae}^2}{v_{\rm k}^2}\frac{\alpha_{\rm f}^2 - 1}{\alpha_{\rm f}^2} \right] \\ &= 2\pi L \frac{1}{8} R^2 w^2 \left[\rho_{\rm i}\frac{v_{\rm k}^2 + v_{\rm Ai}^2}{v_{\rm k}^2} + \rho_{\rm e}\frac{v_{\rm k}^2 + v_{\rm Ae}^2}{v_{\rm k}^2}(1 - f) \right] \\ &= \pi R^2 L \left\{ \frac{1}{2}(\rho_{\rm i} + \rho_{\rm e}) w^2 - f\frac{1}{4}\rho_{\rm e}\frac{v_{\rm k}^2 + v_{\rm Ae}^2}{v_{\rm k}^2} w^2 \right\}. \end{aligned} \tag{10}$$

The rightmost term (which is proportional to f) in the above equation will be dropped from further analysis. This term is the energy contained outside of the cylinder with radius d_f. This term will be of the same magnitude as the additional energy (which is not included in our model) due to the interaction of neighboring loops. Indeed, we have assumed that there is a cylinder of radius d_f around each structure where the wave behavior is only determined by that plasma structure. Taking into account the interaction (see, e.g., Luna et al. 2008; Van Doorsselaere et al. 2008c; Gijsen & Van Doorsselaere 2014) would change the eigenfunction near $r = d_f$, where the solution would change from an "exponential decay" into a "hyperbolic cosine" (of course modified by the geometry). This correction is also of the order of the filling factor, f, and would be of comparable size to the additional term in Equation (10). In conclusion, we can safely neglect the higher order term in Equation (10), because it is of the same magnitude as effects that have not been included in our model. In practice, this means that we are restricted to loop ensembles with low filling factors.

Let us assume that the filling factor, f, is much smaller than one ($f \ll 1$, say $f \lesssim 10\%$). In the first order approximation (for small f), we thus obtained that the total energy in the kink wave is given by

$$E_{\rm Kw} = \left(\pi R^2 L\right) \frac{1}{2}(\rho_{\rm i} + \rho_{\rm e}) w^2. \tag{11}$$

By using Equation (2) for d_f in Equation (6), we thus find

$$E_{\rm bAw} = \frac{1}{f} \frac{\rho}{\rho_{\rm i} + \rho_{\rm e}} E_{\rm Kw} \tag{12}$$

as a direct relation between the total energy of the bulk Alfvén wave and the kink wave in the same cross-section of the cylindrical volume. In this equation, it is understood that w is the same (observed) amplitude for both the Alfvén and kink wave models.

4. OBSERVATIONS

4.1. Connecting the Energy Flux to the Filling Factor

When observing transverse waves in the corona, the energy flux, F, (with physical units of W m^{-2}) can be estimated from the fact that energy ε (energy density J m^{-3}) is propagated at the group speed ($v_{\rm gr}$):

$$F = \varepsilon v_{\rm gr}. \tag{13}$$

In this expression, both the energy flux, F, and the energy density, ε, are, in general, functions of position (particularly in the cross-sectional plane). In an interpretation in terms of Alfvén waves, Equation (5) shows a uniform energy density, $\varepsilon_{\rm bAw}$, and consequently a uniform energy flux, $F_{\rm bAw}$. With the use of that equation, one immediately arrives at the relation

$$F_{\rm bAw} = \frac{1}{2} \rho w_{\rm obs}^2 v_{\rm gr}. \tag{14}$$

When observing transverse waves in the corona, the observed energy flux, $F_{\rm obs}$, is usually estimated with this classic formula.

While obtaining Equations (5) and (14) it was implicitly assumed that the wave amplitude, $w_{\rm obs}$, and the plasma density, ρ, are constant throughout the whole volume. For a kink wave, this is not a good approximation. Instead, we should use Equation (11) to estimate the energy in the kink wave, because the energy density is localized in that case. Thus, to allow comparison between the kink wave and Alfvén wave description, we must obtain an equivalent relation to Equation (14) for kink waves, replacing energy flux and energy density with spatially averaged values. The appropriate average energy density, $\langle \varepsilon_{\rm Kw} \rangle$, is obtained by considering the total energy, $E_{\rm Kw}$, (Equation (11)) normalized by the occupied (on average) volume $V = \pi d_f^2 L = \pi R^2 L / f$, resulting in

$$\langle \varepsilon_{\rm Kw} \rangle = \frac{1}{2} f (\rho_{\rm i} + \rho_{\rm e}) w_{\rm obs}^2. \tag{15}$$

Using this expression in Equation (13) yields the desired formula, expressing the energy propagating in kink modes in a bundle of loops with density filling factor f:

$$F_{\rm obs} = \frac{1}{2} f (\rho_{\rm i} + \rho_{\rm e}) w_{\rm obs}^2 v_{\rm gr}. \tag{16}$$

This assumes that the observed amplitudes, $w_{\rm obs}$, are the peak amplitudes at the loop cores (and not the rms amplitude). Thus, from Equations (14) and (16), the energy flux according to the kink mode interpretation as compared to the Alfvén mode interpretation follows the same rule as the energy (Equation (12)):

$$F_{\rm Kw} = f \frac{\rho_{\rm i} + \rho_{\rm e}}{\rho} F_{\rm bAw}. \tag{17}$$

The group speed in expressions 14 and 16 can be approximated by the observed phase speed. This is exact for the bulk Alfvén wave, but is also sufficiently accurate for kink waves because they are only weakly dispersive.

Equation (16) is a simple formula for the energy flux (in W m^{-2}) of the kink wave that can serve as a drop-in replacement for the classic formula (Equation (14)) to estimate the energy flux by transverse kink waves in structured media, i.e., with multistranded loops or systems containing multiple flux tubes.

For spectroscopic observations, we can accurately measure the velocity amplitude, $w_{\rm obs}$. For imaging observations, however, the velocity amplitude, $w_{\rm obs}$, is not a direct observable; rather, one observes the transverse displacement amplitude, $\xi_{\rm obs}$. From theory, we know that the velocity amplitude, $w_{\rm Kw}$, is related to the displacement amplitude, $\xi_{\rm Kw}$, by

$$w_{\rm Kw} = \omega_{\rm Kw} \xi_{\rm Kw} = \frac{2\pi}{P_{\rm Kw}} \xi_{\rm Kw}, \tag{18}$$

where P is the period of the studied wave and ω is the frequency. Substituting those expressions into Equation (16), we obtain an expression for the energy in propagating transverse waves that we can use for imaging observations:

$$F_{\rm obs} = \frac{1}{2} f (\rho_{\rm i} + \rho_{\rm e}) \left(\frac{2\pi}{P_{\rm obs}}\right)^2 \xi_{\rm obs}^2 v_{\rm gr}. \tag{19}$$

Because the solar atmosphere is mostly optically thin, it is unfortunately not easy to measure the internal density of the strands, $\rho_{\rm i}$, and the surrounding density, $\rho_{\rm e}$, independently or accurately. However, if one tries to observationally estimate density, ρ, it is usually safe to assume that it is associated with a solar atmospheric structure that stands out from the background (due to the presence of waves or higher intensity). Therefore,

Table 1
Comparison of Relevant Filling Factors and Their Energy Flux Reduction

Filling Factor f	Radius of Region d_f	Energy Flux Multiplier (Range)	Example Configuration
20%	2.2 R	20%–39%	Left panel, Figure 2
10%	3.2 R	10%–20%	Middle panel, Figure 2
4%	5 R	4%–8%	Right panel, Figure 2

it can be considered as a good approximation for ρ_i. With this density estimate, we can calculate the energy flux to be between

$$f\frac{1}{2}\rho_i w_{obs}^2 v_{gr} \leqslant F_{obs} \leqslant 2f\frac{1}{2}\rho_i w_{obs}^2 v_{gr}. \quad (20)$$

The left limit is obtained for strands that are much more dense than the surroundings ($\rho_e \ll \rho_i$) and the right limit is for the other extreme, when the flux tubes have the same density as the surroundings ($\rho_e = \rho_i$).

The formulae (16), (19), and (20) are only valid for small filling factors, f, (say up to 10%), because our model ignores any interaction between neighboring structures. A model for collections of flux tubes with higher filling factors would essentially need to take into account the interaction between neighboring flux tubes. An initial attempt could be made in a two-loop system, using the bicylindrical coordinates (Van Doorsselaere et al. 2008c; Robertson et al. 2010; Robertson & Ruderman 2011; Gijsen & Van Doorsselaere 2014). Ultimately, one would need to calculate the energy flux using the T-matrix formulation that takes into account the interaction in systems of more than two flux tubes (e.g., Bogdan & Cattaneo 1989; Keppens et al. 1994; Luna et al. 2009, 2010).

4.2. Considerations on f

Formula (20) is very well suited to elegantly estimate the energy in transverse waves in a bundle of loops/spicules, because it only requires one observable extra (compared to the estimate by the energy in bulk Alfvén waves). The extra required observable is the filling factor, f, of the density structures.

The filling factor may be estimated spectroscopically. Here we summarize the results from some recent works. Warren et al. (2008) find filling factors of around 10% for active region loops and Landi et al. (2009) find a filling factor of cooling loops in quiescent active regions around 30%. Young et al. (2012) find a filling factor for an active region fan loop between 3% and 30%, but they find values between 10% and 20% in their most reliable pixels. Tripathi et al. (2009) study the dependence of filling factors on the height in the atmosphere and the spectral line used. Using the spectral line of Fe XII, they find filling factors ranging from 2% at the loop footpoints to 80% at a height of 40 Mm. Using other spectral lines at the same location, they find filling factors close to 100% (with Mg VII), or exceeding 100% (with Si X). However, the authors state that the spectroscopic determination of filling factors depends on a good background subtraction and a reliable estimate of the width of the emitting structure and, as a consequence, the errors in the above measurements are rather large.

In the chromosphere, the filling factor of spicules has also been observationally estimated. Makita (2003) found a filling factor of 5% at a height of 4 Mm using the Ca H & K lines in eclipse observations. Klimchuk (2012) estimated the filling factor of spicules in the quiet sun to be less than 4.5% and even lower in active regions. Using Hα observations with the ROSA instrument, Morton et al. (2012) found an upper limit filling factor of open chromospheric structures (i.e., connecting to higher layers and thus important for energy propagation) to be 4%–5%.

As an alternative, the filling factor could be estimated by using the mean interloop/interspicule distance (e.g., by using Equation (2)). As a starting point, we state that several recent observations of loops/spicules in groups have an apparent interstructure distance of about one tube width, see, e.g., Figure 2 (top, middle panel) and Figure 4 in Morton & McLaughlin (2013) for coronal loops and Figure 2B (bottom right corner) in De Pontieu et al. (2007) for spicules. However, an intertube distance of about one tube diameter can be the result of several three-dimensional (3D) configurations (that have been integrated over the line of sight).

To make further progress, we consider several grid-like loop ensembles in Figure 2 that are schematic representations of possible 3D configurations. All of the displayed tube grids have a common feature: both the side and top views (integrated over the line of sight) result in images with an intertube distance of a tube diameter 2 R.

For these simple configurations, it is easy to calculate the filling factor. In each configuration, it is possible to find a common repeating square tile centered on a specific cylinder. These square tiles are indicated with dashed lines in Figure 2. In order to calculate the filling factor, one can take the ratio of the surface of the circle with radius R and the square tile with the indicated half side. For example, for the most tightly packed configuration (left panel), we obtain a filling factor of

$$f = \frac{\pi R^2}{(4R)^2} = \frac{\pi}{16} \approx 20\%. \quad (21)$$

The filling factors of the middle and rightmost configurations are, respectively, 10% and 4%.

From these simple models, we can conclude that the filling factor is probably not very high when, as a constraint, a 2D projection has an interloop spacing with the width of one loop. In our idealized cases, we find $f \lesssim 20\%$ as an extreme value, but cases with filling factors less than 10% seem equally likely. These values based on a simple mathematical model agree reasonably with the (wide-spread) spectroscopically measured values that were discussed at the start of this subsection. The resulting reduction in wave energy flux using our proposed formula (compared to the bulk Alfvén wave formula) is summarized in Table 1.

5. CONCLUSIONS

Van Doorsselaere et al. (2008a) discussed the properties of transverse waves in a coronal plasma with a structure transverse to the magnetic field. They stated that a kink wave formalism is perhaps more appropriate to describe the transverse waves observed in chromospheric and coronal structures, because that formalism takes into account the density structuring transverse to the magnetic field. Van Doorsselaere et al. stated this would be important, because seismologically estimated values for the

magnetic field could differ up to 50% by using an Alfvén wave interpretation.

In their paper, Van Doorsselaere et al. state another important consequence of the difference between bulk Alfvén waves and kink waves. They hypothesized that the energy content in transverse kink waves is drastically reduced compared to a description in terms of bulk Alfvén waves. Their hypothesis was that the energy content would be reduced by the density filling factor. Until now, this statement had not been quantified.

In this paper, we have for the first time calculated the propagating energy in an ensemble of cylindrical structures using a density filling factor. To that end, we have used the formulae introduced by Goossens et al. (2013a, 2013b) who calculated the energy content in a kink wave in a standalone cylindrical structure. We have generalized their work by linking their formulae to the filling factor of the underlying density structure.

In this paper, we have proposed a new formula to estimate the energy flux, F, in observed transverse waves. It can be easily calculated by

$$f\frac{1}{2}\rho_{\rm i}w_{\rm obs}^2 v_{\rm gr} \leqslant F = f(\rho_{\rm i}+\rho_{\rm e})\frac{1}{2}w_{\rm obs}^2 v_{\rm gr} \leqslant 2f\frac{1}{2}\rho_{\rm i}w_{\rm obs}^2 v_{\rm gr}, \quad (22)$$

where the left and right equalities are satisfied in the high- and low-density contrast limits, respectively. In this formula, ρ is an observed density of the oscillating structure, f is the density filling factor, $w_{\rm obs}$ is the observed transverse velocity amplitude, and $v_{\rm gr}$ is the measured group speed.

With this formula, we have thus confirmed the hypothesis by Van Doorsselaere et al. (2008a). Indeed, the energy flux in kink waves is the energy flux of bulk Alfvén waves, multiplied with a correction factor between f and $2f$, where f is the filling factor of the density structure. Our formula can be used as a drop-in replacement for the classical formula for the energy in bulk Alfvén waves, allowing for a convenient way to measure the energy flux in observed transverse waves.

We have calculated the correction to the energy flux for three representative grid-like configurations (with filling factors of 20%, 10%, and 4%). The corrections to the energy flux (in comparison to the expression for bulk Alfvén waves) are 20%–39%, 10%–20% and 4%–8%, respectively.

Of course, in this paper, we have assumed that all observed wave properties (amplitude and group speed) have been measured correctly. However, it was shown by De Moortel & Pascoe (2012) that the line-of-sight integration of the intensity could lead to a drastic reduction of the measured wave amplitude when using spectroscopic observations (such as the CoMP observations, Tomczyk et al. 2007). With their numerical simulation, they showed that spectroscopic observations could underestimate the available energy. This effect is in competition with our model, where we propose that the observed wave flux should be multiplied (reduced) with the density filling factor.

Nevertheless, our formula for the energy flux can be directly applied to the energy fluxes reported by De Pontieu et al. (2007); McIntosh et al. (2011); Thurgood et al. (2014) who used imaging observations. The energy flux estimates in those papers were done with the classic Alfvén wave formula (Equation (14)), because no appropriate formula was available at that time. Not taking into account updated wave amplitude estimates (Okamoto & De Pontieu 2011), the energy flux in transverse waves in chromospheric spicules of 4–7 kW m^{-2} reported by De Pontieu et al. (2007) would be recalculated with our improved formula to 200–700 W m^{-2}, assuming a spicule density filling factor of 5%. These values agree rather well with the energy flux of transverse waves found by Morton et al. (2012), who did take into account the filling factor. Likewise, the energy flux estimates in transverse waves in coronal loops of 100 W m^{-2} reported by McIntosh et al. (2011) (who calculated the energy flux using a "wave filling factor" of 100%) would be reduced to 10–20 W m^{-2}, using a density filling factor of 10% for their observed loop bundle. In this recalculation, we have not taken into account the claim of Morton & McLaughlin (2013) that the velocity amplitudes measured with Hi-C are smaller than the one used in McIntosh et al. (2011). In the recent paper by Thurgood et al. (2014), the reported energy flux of transverse waves in polar plumes of 9–24 W m^{-2} would be lowered to 0.9–4.8 W m^{-2} with our formula, again, using a density filling factor of 10%.

We are grateful to Marcel Goossens for interesting discussions regarding the subject of this paper. The research leading to these results has been sponsored by an Odysseus grant of the FWO Vlaanderen. It has been performed in the context of the IAP P7/08 CHARM (Belspo) and the GOA-2015-014 (KU Leuven). T.V.D. acknowledges the funding from the FP7 ERG grant no. 276808. G.V. greatly appreciates the support of the Leverhulme Trust (UK).

REFERENCES

Andries, J., Arregui, I., & Goossens, M. 2005, ApJL, 624, L57
Arregui, I., Andries, J., Van Doorsselaere, T., Goossens, M., & Poedts, S. 2007, A&A, 463, 333
Aschwanden, M. J., Fletcher, L., Schrijver, C. J., & Alexander, D. 1999, ApJ, 520, 880
Aschwanden, M. J., Nightingale, R. W., Andries, J., Goossens, M., & Van Doorsselaere, T. 2003, ApJ, 598, 1375
Asensio Ramos, A., & Arregui, I. 2013, A&A, 554, A7
Bogdan, T. J., & Cattaneo, F. 1989, ApJ, 342, 545
Bogdan, T. J., & Zweibel, E. G. 1987, ApJ, 312, 444
Cirtain, J. W., Golub, L., Lundquist, L., et al. 2007, Sci, 318, 1580
De Moortel, I., & Pascoe, D. J. 2012, ApJ, 746, 31
De Pontieu, B., McIntosh, S. W., Carlsson, M., et al. 2007, Sci, 318, 1574
Edwin, P. M., & Roberts, B. 1983, SoPh, 88, 179
Erdélyi, R., & Fedun, V. 2007, Sci, 318, 1572
Fujimura, D., & Tsuneta, S. 2009, ApJ, 702, 1443
Gijsen, S. E., & Van Doorsselaere, T. 2014, A&A, 562, A38
Goossens, M., Andries, J., & Aschwanden, M. J. 2002, A&A, 394, L39
Goossens, M., Andries, J., Soler, R., et al. 2012a, ApJ, 753, 111
Goossens, M., Arregui, I., Ballester, J. L., & Wang, T. J. 2008, A&A, 484, 851
Goossens, M., Soler, R., Arregui, I., & Terradas, J. 2012b, ApJ, 760, 98
Goossens, M., Terradas, J., Andries, J., Arregui, I., & Ballester, J. L. 2009, A&A, 503, 213
Goossens, M., Van Doorsselaere, T., Soler, R., & Verth, G. 2013a, ApJ, 768, 191
Goossens, M., Van Doorsselaere, T., Soler, R., & Verth, G. 2013b, ApJ, 771, 74
He, J., Marsch, E., Tu, C., & Tian, H. 2009a, ApJL, 705, L217
He, J.-S., Tu, C.-Y., Marsch, E., et al. 2009b, A&A, 497, 525
Keppens, R., Bogdan, T. J., & Goossens, M. 1994, ApJ, 436, 372
Klimchuk, J. A. 2012, JGRA, 117, 12102
Landi, E., Miralles, M. P., Curdt, W., & Hara, H. 2009, ApJ, 695, 221
Luna, M., Terradas, J., Oliver, R., & Ballester, J. L. 2008, ApJ, 676, 717
Luna, M., Terradas, J., Oliver, R., & Ballester, J. L. 2009, ApJ, 692, 1582
Luna, M., Terradas, J., Oliver, R., & Ballester, J. L. 2010, ApJ, 716, 1371
Makita, M. 2003, PNAOJ, 7, 1
McIntosh, S. W., de Pontieu, B., Carlsson, M., et al. 2011, Natur, 475, 477
Moreels, M. G., & Van Doorsselaere, T. 2013, A&A, 551, 137
Morton, R. J., & McLaughlin, J. A. 2013, A&A, 553, L10
Morton, R. J., Verth, G., Fedun, V., Shelyag, S., & Erdélyi, R. 2013, ApJ, 768, 17
Morton, R. J., Verth, G., Jess, D. B., et al. 2012, NatCo, 3, 1315

Nakariakov, V. M., & Ofman, L. 2001, A&A, 372, L53
Nakariakov, V. M., Ofman, L., DeLuca, E. E., Roberts, B., & Davila, J. M. 1999, Sci, 285, 862
Okamoto, T. J., & De Pontieu, B. 2011, ApJL, 736, L24
Pasachoff, J. M., Noyes, R. W., & Beckers, J. M. 1968, SoPh, 5, 131
Pascoe, D. J., Wright, A. N., & De Moortel, I. 2010, ApJ, 711, 990
Robertson, D., & Ruderman, M. S. 2011, A&A, 525, A4
Robertson, D., Ruderman, M. S., & Taroyan, Y. 2010, A&A, 515, A33
Schrijver, C. J., Title, A. M., Berger, T. E., et al. 1999, SoPh, 187, 261
Spruit, H. C. 1982, SoPh, 75, 3
Thurgood, J. O., Morton, R. J., & McLaughlin, J. A. 2014, ApJL, 790, L2
Tomczyk, S., & McIntosh, S. W. 2009, ApJ, 697, 1384
Tomczyk, S., McIntosh, S. W., Keil, S. L., et al. 2007, Sci, 317, 1192
Tripathi, D., Mason, H. E., Dwivedi, B. N., del Zanna, G., & Young, P. R. 2009, ApJ, 694, 1256
van der Holst, B., Sokolov, I. V., Meng, X., et al. 2014, ApJ, 782, 81
Van Doorsselaere, T., Nakariakov, V. M., & Verwichte, E. 2008a, ApJL, 676, L73
Van Doorsselaere, T., Nakariakov, V. M., Young, P. R., & Verwichte, E. 2008b, A&A, 487, L17
Van Doorsselaere, T., Ruderman, M. S., & Robertson, D. 2008c, A&A, 485, 849
Vasheghani Farahani, S., Van Doorsselaere, T., Verwichte, E., & Nakariakov, V. M. 2009, A&A, 498, L29
Verdini, A., Grappin, R., Pinto, R., & Velli, M. 2012, ApJL, 750, L33
Verth, G., Terradas, J., & Goossens, M. 2010, ApJL, 718, L102
Verwichte, E., Van Doorsselaere, T., White, R. S., & Antolin, P. 2013, A&A, 552, A138
Walker, A. 2005, Magnetohydrodynamic Waves in Geospace: The Theory of Ulf Waves and Their Interaction with Energetic Particles in the Solar-Terrestrial Environment (Series in Plasma Physics; Bristol, UK: Institute of Physics)
Warren, H. P., Ugarte-Urra, I., Doschek, G. A., Brooks, D. H., & Williams, D. R. 2008, ApJL, 686, L131
Wentzel, D. G. 1979a, ApJ, 227, 319
Wentzel, D. G. 1979b, A&A, 76, 20
Wilson, P. R. 1979, A&A, 71, 9
Wilson, P. R. 1980, A&A, 87, 121
Young, P. R., O'Dwyer, B., & Mason, H. E. 2012, ApJ, 744, 14
Zaitsev, V. V., & Stepanov, A. V. 1975, IGAFS, 37, 3
Zaqarashvili, T. V., Khutsishvili, E., Kukhianidze, V., & Ramishvili, G. 2007, A&A, 474, 627